LS-100
August 1987
Y. Jin
S. L. Kramer

A Study of Closed Orbit Distortions and their Correction for the APS

Y. Jin and S. L. Kramer

Closed orbit distortions (COD) are unavoidable in accelerator due to magnet construction errors and misalignments. With sextupoles or other nonlinear elements in the accelerator, the COD's in these elements cause additional focusing and tune shift for the small amplitude betatron oscillations At larger amplitudes the COD's in non-linear elements could contribute to resonant terms which will limit the dynamic aperture.

The COD's are mainly produced by the following errors:

Quadrupole misalignment errors - $\Delta x_i, \Delta y_i$
Dipole field errors - $(\Delta B\ell/B\ell)_i$
Dipole axial roll errors - $(\Delta\phi)_i$

where i stands for any one element. These errors are modeled by randomly distributed Gaussian errors with a mean of zero and an rms value given by: Δx, Δy, $\Delta B\ell/B\ell$, and $\Delta\phi$. For the Advanced Photon Source (APS) the tolerances (rms value) on these errors are specified to be

Δx, $\Delta y = 10^{-4}$ meter
$\Delta B\ell/B\ell = 10^{-4}$
$\Delta\phi = 10^{-4}$ radian.

For this tolerance level, the average dynamic aperture for the APS lattice decreased from $(N_x \times N_y) = (85 \times 85)$ to $\simeq (40 \times 40)$. However, correction magnets can be introduced into the lattice and tuned to reduce the COD's in the lattice. This will have the effect of increasing the dynamic aperture and improving other lattice properties (e.g., natural emittance, dispersion, etc.).

A. Generation of Closed Orbit Distortions

The COD's for the storage ring are (to first order) the result of dipole error fields δB, which are not defined in the ideal lattice structure. For small error fields the effect on the closed orbit (relative to the reference orbit) is given by[1]

$$u(s) = \frac{\sqrt{\beta(s)}}{2 \sin \pi \nu} \int \frac{\delta B(s')}{B\rho} \sqrt{\beta(s')} \cos \{\mu(s)-\mu(s') - \pi \nu\} ds' \qquad (1)$$

where u(s) represents either x(s) or y(s) for the horizontal or vertical closed orbit, respectively. The β, ν, and μ are taken for the horizontal and vertical plane for x(s) and y(s), respectively, and δB is the perpendicular field component.

The quadrupole and dipole errors described above contribute to Eq. (1), the Gaussian distributed random field errors with rms values are given by:

$$\left(\frac{\delta B_y \ell}{B\rho}\right)_{rms} = K\ell\Delta x \qquad \text{(quadrupole)}$$

$$= \theta_B \frac{\Delta B\ell}{B\ell} \qquad \text{(dipole)}$$

$$\left(\frac{\delta B_x \ell}{B\rho}\right)_{rms} = K\ell\Delta y \qquad \text{(quadrupole)}$$

$$= \theta_B \Delta\phi \qquad \text{(dipole)},$$

where θ_B = the bend angle of the dipole magnet. The integral in Eq. (1) can be represented by a finite sum over the individual errors. The expectation values for the COD at any point in the lattice can be obtained by using the randomness of the errors to give [1]

$$X_{rms}(s) = \frac{\sqrt{\beta_x(s)}}{2\sqrt{2} \sin \pi \nu_x} \{(\Delta x)^2 \sum_i (K\ell)_i^2 \beta_{x_i} + \left(\frac{\Delta B\ell}{B\ell}\right)^2 \sum_i \theta_B^2 \beta_{x_i}\}^{1/2}$$

$$Y_{rms}(s) = \frac{\sqrt{\beta_y(s)}}{2\sqrt{2} \sin \pi \nu_y} \{(\Delta y)^2 \sum_i (K\ell)_i^2 \beta_{y_i} + \Delta\phi^2 \sum_i \theta_B^2 \beta_{y_i}\}^{1/2} \qquad (2)$$

where the first summation is over all quadrupoles and the second is over all dipoles in the lattice. For the APS with the tolerance level specified above,

the expectation values for the COD averaged over the lattice are

$$\overline{X}_{rms} \approx 5.2 \text{ mm}$$

and

$$\overline{Y}_{rms} \approx 4.2 \text{ mm}$$

with 90% of the contribution to these values from the quadrupoles and only 10% from the dipole magnets.

The effect of a COD (Δx_i) in the sextupoles is a tune shift in the horizontal and vertical arising from the additional focusing strength, δK, in the sextupoles. The tune shift, to first order, is given by

$$\Delta\nu = -\frac{1}{4\pi} \int \beta(s)\ \delta K(s)\ ds \tag{3}$$

or

$$\Delta\nu = -\frac{1}{4\pi} \sum_i \beta_i\ S_i\ \Delta x_i \tag{4}$$

where $\delta(K\ell)_i = \left(\frac{B''\ \ell}{B\rho}\right)_i \Delta x_i = S_i \Delta x_i$ for sextupole i with strength S_i. The effect of the COD in the sextupole on the tune shift can be estimated by considering the tune shift due to random displacements of the closed orbit in the sextupoles. For this case the tune shifts are:

$$(\Delta\nu_x)_{rms} = 40\ \Delta x_{rms}$$

$$(\Delta\nu_y)_{rms} = 67\ \Delta x_{rms},$$

where Δx_{rms} is in units of mm. For a 1 mm random closed orbit in the horizontal, a significant tune shift of $(\Delta\nu_x)_{rms} \approx 0.04$ and $(\Delta\nu_y)_{rms} \approx 0.07$ is produced by the sextupoles. Therefore, the expected tune shift for the specified tolerance levels will have a significant influence on the dynamic aperture.

In addition to tune shifts, the COD's in sextupoles introduce changes in: betatron functions, dispersion, natural emittance and coupling. The program PETROS[2] was used to estimate average and rms values for these properties and are shown in Table I, for the tolerance levels specified above. Similar results are obtained using the programs RACETRACK[3] and MAD[4] (except for emittance and couplings). These last two programs were also used to calculate the dynamic aperture reduction.

B. Closed Orbit Correction

The closed orbit distortions discussed above need not limit the performance of the storage ring since beam position monitors and small dipole correction magnets can be used to reduce the distortions. The ideal correction scheme is to remove the actual errors which produce the closed orbit distortions. This is difficult in practice since all magnets would require five or more jacks capable of 10-μm resolution and shunts capable of 10^{-5} resolution in shunting current for the dipole magnets. Even with this sophistication only the average offsets and errors could be corrected for any one magnet. Consequently correction dipoles are necessary to reduce the closed orbit at certain points in the ring. Since these dipoles are actually tuneable error fields at points different than the existing error fields, they cannot reduce the closed orbit distortions to zero everywhere but only at the certain locations (e.g., monitors).

The reduction in dynamic aperture for the APS is due to the closed orbit distortions in the strong sextupole magnets. Consequently, the beam position monitors are placed as close as possible to the sextupoles, in order to reduce the closed orbits distortion at these locations and therefore their effect on the dynamic aperture. With a sufficient number of correctors, the closed orbit distortions could, in principle, be reduced to zero at the monitors, but will in practice be limited by the available correctors or the alignment error for monitors relative to the center of the sextupoles.

Several methods have been used to calculate the closed orbit correction for the APS. All methods make use of the least squares method to minimize the deviation of the COD from a zero value in all of the correctors. If monitor alignment errors are included, then the COD can only be corrected to minimize the COD deviation in the monitor relative to their randomly distributed alignment error.

The program RACETRACK has a highly efficient 3-bump correction algorithm and was used for all dynamic aperture calculations. This program also has a most efficient corrector algorithm which had a slower convergence (required more iterations) and therefore was not used. Similar dynamic aperture results were obtained with MAD, which uses the MICADO[5] algorithm.

Since the dynamic aperture calculations of MAD were time consuming, this program was used only to check the RACETRACK results. This comparison of the dynamic aperture typically agreed to within 1 mm for the cases studied. The calculation of corrected emittance was done with the program PETROC[6] which also uses the MICADO algorithm.

C. Closed Orbit Correction Schemes

All algorthims are dependent on the number of correctors used in the lattice. For example in the 3-bump method, if too many correctors are provided they are all used in the calculation, and the algorithm doesn't realize that a smaller residual COD could be obtained by setting several corrector strengths to zero. Consequently, a study of the improvement in dynamic aperture has been performed for different arrangements of correction dipoles.

We have calculated more than twenty schemes for the closed orbit correction of APS storage ring. We will compare some results for eight of these schemes. The available correctors and monitors for the APS are shown in Fig. 1. The actual corrector positions for eight schemes (A-H) studied are shown in Fig. 2. The unused monitors and correctors are reserved for photon beam steering. Some of the schemes studied are not possible with the present APS lattice, due to the difficulty of providing vertical dipole fields (horizontal correction) in the sextupole magnets. However, these schemes will provide some guidance as to whether vertical dipole fields are useful and worth the effort to provide. The correction scheme -C is the one proposed for the APS and described in the CDR -'87.[7]

Figures 3 and 4 show the dependence of the residual closed orbit in the monitors as a function of the iteration number for the RACETRACK 3-Bump correction. All correction schemes were iterated four times and the residual rms closed orbit deviation and the maximum corrector strength is shown in Figs. 5 and 6. The schemes with the greatest number of correctors (A & B) have the largest corrector strengths but also do not have the smallest residual closed orbit. For the schemes with the least number of correctors, there are insufficient correctors to yield a small residual closed orbit.

When random errors are introduced into a lattice, it is necessary to generate a number of different arrangements of errors (different machines), in

order to study the average and rms values for certain properties of the lattice for the different schemes. For this study of closed orbit correction schemes, six machines are generated for each scheme and four iterations of the correction algorithm were calculated for each machine. Figures 7 and 8 show the resulting average and rms spread for the corrected tunes and dynamic aperture for these schemes. The greatest correction of the dynamic aperture is for schemes C, D, and E, which differ very little from the ideal dynamic aperture. Little differences between the schemes are noted for the corrected horizontal tunes and only slightly improved vertical tunes for the C, D, and E schemes.

The above closed orbit calculations were performed with zero monitor alignment error. However, little effect on tunes or dynamic aperture are observed by setting a 0.1 mm monitor error. This is due to the fact that the iterations were stopped for residual closed orbit distortions of about this same level, rather than iterating the correction for a very large number of corrections. Figure 9 shows the result of adding 0.1 mm and 0.5 mm monitor alignment error on the residual closed orbit values.

The influence of the different correction schemes on the natural emittance was studied for one machine (the same for each scheme) using the program PETROC The result is shown in Fig. 10. All schemes were able to correct the natural emittance to better than a 1% increase in the horizontal and coupling, $k < 10^{-3}$.

The results of the corrected closed orbit on the dynamic aperture and natural emittance are summarized in Table 2.

D. The Proposed Closed Orbit Scheme

The scheme C was proposed for the closed orbit correction scheme for the APS.[7] Although schemes D and E had fewer correctors and slightly greater dynamic aperture, this advantage was not sufficient to justify the design of vertical dipole fields (for horizontal orbit correction) in the sextupoles (a difficult job with the present vacuum chamber design).

Figure 11 shows the COD values at the monitors before and after correction and Fig. 12 shows the angular kick for the correction dipoles necessary to correct the closed orbit in Fig. 11. The designed maximum

corrector strenth is four times the peak required for this scheme and the specified tolerance level. This should provide adequate reserve for handling errors larger than the tolerance level and for aperture and tuning studies.

References

1. E. Keil, CERN 77-13, P.52 (1977)

2. K. Steffen, J. Kewich, DESY PET - 76109, (1976).

3. A. Wrulich, DESY 84-26 (1984).
   S. Kramer, ANL Light Source note LS-67.
   H. Nishimura (LBL), private communication.

4. F. Iselin, J. Niederer, CERN/LEP-TH/87-33 (1987).

5. B. Autin, Y. Marti, CERN ISR-MA/73-17 (1973).

6. G. Guignard, Y. Marti, CERN/ISR-BOM-TH/81-32 (1981).

7. 7-GEV Advanced Photon Source, Conceptual Design Report, ANL-87-15 (1987).

Table I.
Uncorrected lattice functions for APS Lattice

Tolerance level Program (# Machine studied)		No Errors PETROS	10^{-4} level PETROS (20 machines)	10^{-4} level RACETRACK (10 machines)	10^{-4} level MAD (10 machines)	
Tunes	ν_x	0.2159	0.259±0.045	0.184±0.040	0.158±0.029	
	ν_y	0.2984	0.322±0.020	0.314±0.018	0.320±0.018	
Undulator	β_x	13	13.3±2.4	15.4±7.3	12.3±2.6	m
	β_y	10	10.1±1.7	10.1±1.3	10.5±1.4	m
	D_x	0	-0.007±0.046	-0.010±0.3	0.021±0.18	m
	D_y	0	-0.004±0.008	-0.0±0.01	0.0	m
Emittance	ε_x	7.95	9.4±3.2	-	-	nm
	ε_y	0	0.97±1.2	-	-	nm
	$k = \frac{\varepsilon_y}{\varepsilon_x}$	0	0.1±0.16	-	-	
	$\varepsilon_n = \varepsilon_x + \varepsilon_y$	7.95	10.4±3.9	-	-	nm
COD at sextupole						
	X_{rms}	0	3.93	4.64	5.32	mm
	δX_{rms}	0	1.81	2.99	1.90	mm
	Y_{rms}	0	3.22	3.29	4.05	mm
	δY_{rms}	0	1.06	1.25	0.73	mm
Dynamic Aperture						
(σ_x=0.322 σ_y=0.199)						
	$N_x = N_y$	85×85	-	38×38 ±10	32×32 ±8	
Stable/Machines		-	20	10	10	

Table 2
Comparison of Corrected Lattice Properties for Different Schemes

Scheme	RMS COD in Monitors X(mm)	Y(mm)	Corrected Tunes ν_x	ν_y	Dynamic Aperture $N_x=N_y$	Max.Corr. Strength (mrad)	Corrected Emittance* $\varepsilon_x(10^{-9}m)$	$\varepsilon_y(10^{-10}m)$	$k = \frac{\varepsilon_y}{\varepsilon_x}(\%)$
A (σ_m=0)	0.23±0.10	0.14±0.04	0.214±0.002	0.307±0.007	64±3	1.13	8.00	0.03	0.04
B (σ_m=0)	0.23±0.09	0.07±0.008	0.215±0.001	0.306±0.006	68±5	1.12	7.99	0.12	0.15
C (σ_m=0)	0.05±0.002	0.07±0.008	0.216±0.002	0.298±0.003	81±5	0.32	7.99	0.13	0.16
C (σ_m=0.1 mm)	0.07±0.001	0.09±0.007	0.213±0.002	0.296±0.003	82±2	0.32	-	-	-
C (σ_m=0.5 mm)	0.28±0.001	0.26±0.002	0.202±0.002	0.288±0.003	70±2	0.31	-	-	-
D (σ_m=0)	0.02±0.001	0.07±0.009	0.216±0.001	0.299±0.002	86±2	0.21	7.99	0.10	0.13
D (σ_m=0.1 mm)	0.06±0.001	0.09±0.007	0.213±0.001	0.295±0.002	82±2	0.21	-	-	-
E (σ_m=0)	0.02±0.001	0.07±0.01	0.216±0.001	0.299±0.002	85±3	0.21	8.00	0.06	0.08
F (σ_m=0)	0.18±0.02	0.08±0.01	0.208±0.008	0.285±0.013	77±5	0.24	7.97	0.04	0.05
G (σ_m=0)	0.36±0.04	0.08±0.01	0.216±0.006	0.301±0.009	69±5	0.30	8.01	0.05	0.06
H (σ_m=0)	0.36±0.04	0.27±0.03	0.216±0.006	0.301±0.009	64±5	0.30	7.90	1.20	1.52

*Corrected emittance calculated for one machine using PETROC.
All other results are for 6 machines using RACETRACK 3-bump correction.
σ_m is the monitor alignment tolerance assumed.

APPENDIX A
CLOSED ORBIT CORRECTION METHODS

In a storage ring with m monitors and n correctors, the corrector strengths θ_i (i = 1,2, ...n) are adjusted in order to set the measured values of the closed orbit x_j (j = 1,2,...m) to zero. The change in the closed orbit at monitor j due to turning on the corrector i to the values θ_i is given to first order by

$$\Delta x_j = \sum_{i=1}^{n} T_{ji}\, \theta_i$$

where

$$T_{ji} = \frac{\sqrt{\beta_j \beta_i}}{2 \sin \pi\nu} \cos \left[\phi(j) - \phi(i) - \pi\nu\right] .$$

With an insufficient number correctors, the corrected closed orbit cannot be set to zero at all monitors. One method for setting corrector strengths is to minimize the sum of the square of the corrected closed orbit deviations from zero at all monitors. The sum of the squares

$$F = \sum_{j=1}^{m} x_j^2$$

with $x_j = x_{oj} + \Delta x_j$ for x_{oj} = initial COD value, has a minimum for θ_i given by

$$\frac{\partial F}{\partial \theta_i} = 0$$

for all i = 1,2,...n. The values θ_i are given by the matrix equation

$$\vec{\theta} = - C^{-1} \vec{A}$$

where $$C_{ik} = \sum_{j=1}^{m} T_{ji} T_{jk} \text{ and } A_k = \sum_{j=1}^{m} T_{jk} x_{oj}$$

for (i,k = 1,2,...n).

The MICADO algorithm solves this by using the minimum number of available correctors necessary to provide a peak-to-peak variation of the corrected COD's at the monitors less than some desired value. This is done using orthogonal transformations as described in the original reference.[5]

In RACETRACK, the most significant corrector algorithm searches for the one corrector in the n available which yields the minimum value for F_ℓ. For only one corrector, ℓ, the minimum for F is found directly by

$$\theta_\ell = \frac{-\sum_j T_{j\ell} x_{oj}}{\sum_j |T_{j\ell}|^2} \qquad \text{(A-1)}$$

Then θ_ℓ is used to calculate F_ℓ for $\ell = 1, \ldots n$ and then only one corrector k is set to θ_k for k equal to that value of ℓ which yields the minimum F_ℓ. After setting θ_k, the closed orbit is recalculated (since T_{ji} are linearizations of the actual closed orbit dependence on θ_j) and the procedure iterated. Since only one corrector is changed for each iteration, the convergence is slow.

RACETRACK has a very efficient 3-bump correction algorithm which has been used in this study. This method uses 3 correctors (consecutive if the phase advance between correctors is greater than $0.075 * 2\pi$) to reduce the COD at monitors between the 1st and 3rd. The three correctors are powered in such a way that the closed orbit is unaffected outside the three correctors. If the first corrector is set to θ_1, in order to minimize the sum of the square of the closed orbit deviations at the monitors in between the first and third correctors, then the other correctors must be set to

$$\theta_2 = -\sqrt{\frac{\beta_1}{\beta_2}} \frac{\sin(\phi_3-\phi_1)}{\sin(\phi_3-\phi_2)} \theta_1 \qquad \text{(A-2)}$$

$$\theta_3 = \sqrt{\frac{\beta_1}{\beta_3}} \frac{\sin(\phi_2-\phi_1)}{\sin(\phi_3-\phi_2)} \theta_1 \qquad \text{(A-3)}$$

where β_i and ϕ_i are the beta value and phase advance at corrector i.

For monitors $j = 1,2,\ldots m_1$ in between correctors 1 and 2, the change in the COD at that monitor is

$$\Delta X_j = R_{j1}\theta_1 \qquad (j = 1,2,\ldots m_1)$$

where $$R_{j1} = \sqrt{\beta_j\beta_1}\,\sin(\phi_j-\phi_1)\ .$$

For monitors $j = m_1 + 1,\ m_1 + 2,\ldots m_2$ in between correctors 2 and 3 the change in the COD at that monitor is

$$\Delta X_j = R_{j1}\theta_1 + R_{j2}\theta_2 \quad (j = m_1 + 1,\ldots m_2)$$

where $R_{j2} = \sqrt{\beta_j\beta_2}\sin(\phi_j-\phi_2)$

Using the relationship between θ_2 and θ_1 (Eq. A-2), ΔX_j can be expressed in terms of only θ_1. This yields the relation for all monitors given by

$$\Delta X_j = R'_{j1}\ \theta_1$$

where $$R'_{j1} = R_{j1} \text{ for } (j = 1,2,\ldots m_1)$$

and $R'_{j1} = R_{j1} - \sqrt{\beta_j\beta_1}\,\dfrac{\sin(\phi_3-\phi_1)}{\sin(\phi_3-\phi_2)}\,\sin(\phi_j-\phi_2)$ for $(j = m_1+1,\ m_1+2,\ldots m_2)$.

Then θ_1 can be found by Equation (A-1) with $T_{j\ell}$ replaced by R'_{j1} and θ_2 and θ_3 follow from Eqs. (A-2) and (A-3).

APPENDIX B
MONITOR ALIGNMENT PROCEDURE

The alignment of the electrical center of the beam position monitor relative to the magnetic center of the sextupole will be done by measuring the centers in the laboratory and pinning the monitors to the sextupoles, to maintain their relative position. Despite this careful alignment procedure, a relataive misalignment of these two centers could be as great as ±0.5 mm.

Improvement of the alignment accuracy can be achieved by measuring the relative offset between the sextupole and its monitor with beam. This will be done by varying the strength of one sextupole at a time and measuring the tune shift induced by the offset of the closed orbit in the sextupole. Equation (4) yields a tune shift in a typical sextupole for a 1-mm COD in the sextupole of

$$\Delta\nu = \frac{-\beta}{4\pi} S\, \Delta x \approx 3.7 \times 10^{-3}.$$

By varying the sextupole strength for only one sextupole at a time, the slope of the tune shift can be measured

$$\frac{d\nu}{ds} = \frac{-\beta\Delta x}{4\pi} \approx -\Delta x.$$

Even with considerable uncertainty in β, the point Δx_m where the slope is zero can be estimated by fitting for the point Δx where the slope is zero. The resolution on the slope will depend on the uncertainty in the tune measurement. If the tune spread due to quadrupole ripple and residual chromaticity is less than 10^{-3}, the uncertainty in $\Delta\nu$ will be $\approx 10^{-3}$ for a single measurement. By varying the sextupole strength up to ±20%, the uncertainty in the slope will be $\pm 3 \times 10^{-4}$ m^2. If Δx is varied by ±1 mm (using a local bump) and 9 measurements are made, then the uncertainty in the point Δx_m, where the slope $d\nu/ds$ is zero, can be known to an uncertainty of ±0.11 mm.

This proceaure, although straight forward, will be rather tedious for 280 monitors and sextupoles. This will necessitate a computerized alignment procedure which could yield greater accuracy in Δx_m, by averaging

over many measurements, limited only by the ±0.03 mm resolution of the monitors.

The above procedure only works for the horizontal misalignment, since the vertical offset in the normal sextupoles contribute to a coupling between the horizontal planes. Although conceptually more difficult to handle the above analysis can be performed in the orthogonal eigenplanes and then transformed back to the horizontal and vertical offsets. The uncertainty will certainly increase, especially for the vertical plane. The sensitivity to vertical misalignment and improvements that might be achieved by using skew quadrupole to rotate the eigenplanes will be considered elsewhere.

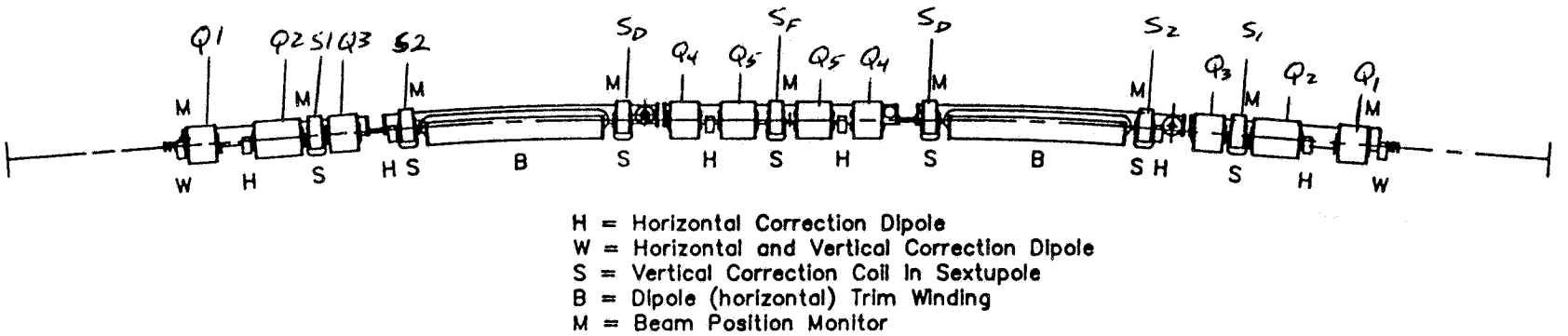

Figure 1. Monitors and correction dipole for one cell of the storage ring.

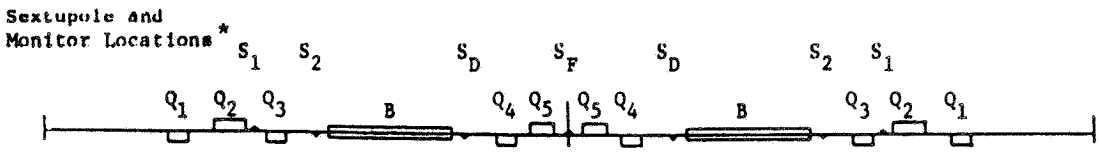

Scheme	Corrector Position											No. horiz. and vert. correctors
	1	2		3	4	5	6	7		8	9	
A	CH	CH		CH		CH		CH		CH	CH	7
	CV	CV		CV				CV		CV	CV	6
B		CH		CH		CH		CH		CH		5
		CV		CV				CV		CV		4
C		CH			CH		CH			CH		4
		CV		CV				CV		CV		4
D	CH					CH					CH	3
		CV		CV				CV		CV		4
E	CH					CH					CH	3
		CV						CV				2
F	CH										CH	2
		CV								CV		2
G						CH						1
		CV								CV		2
H						CH						1
				CV								1

* 7 monitors located next to the sextupole were used for all correction schemes.
CH - Horizontal Corrector
CV - Vertical Corrector

Fig. 2. Location of Monitors and Correctors for the Correction Schemes Studied

Figure 3. RMS horizontal COD at the monitors vs. iteration number for RACETRACK 3-bump method.

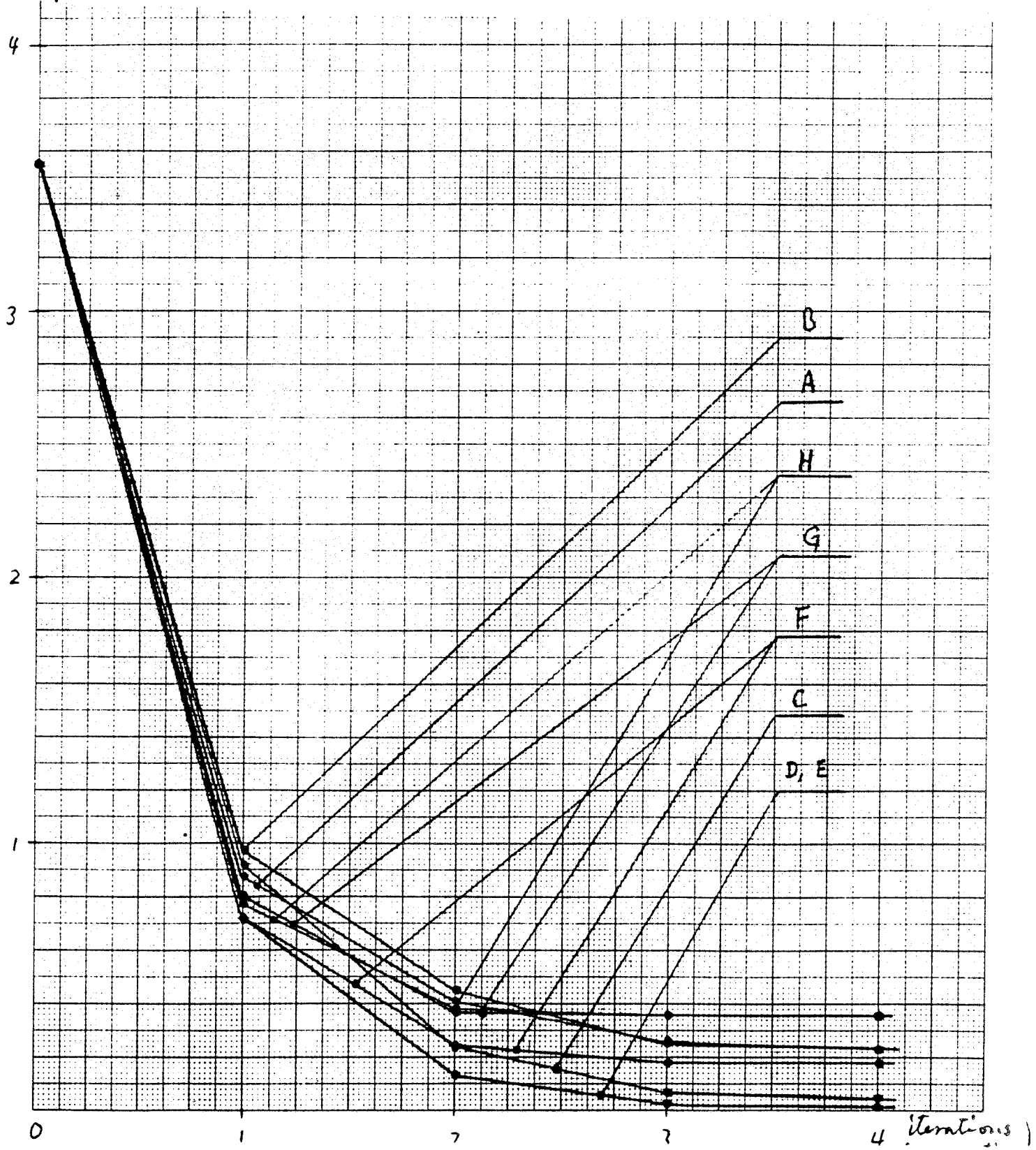

Figure 4. RMS vertical COD at the monitors vs. iteration number for RACETRACK 3-bump method.

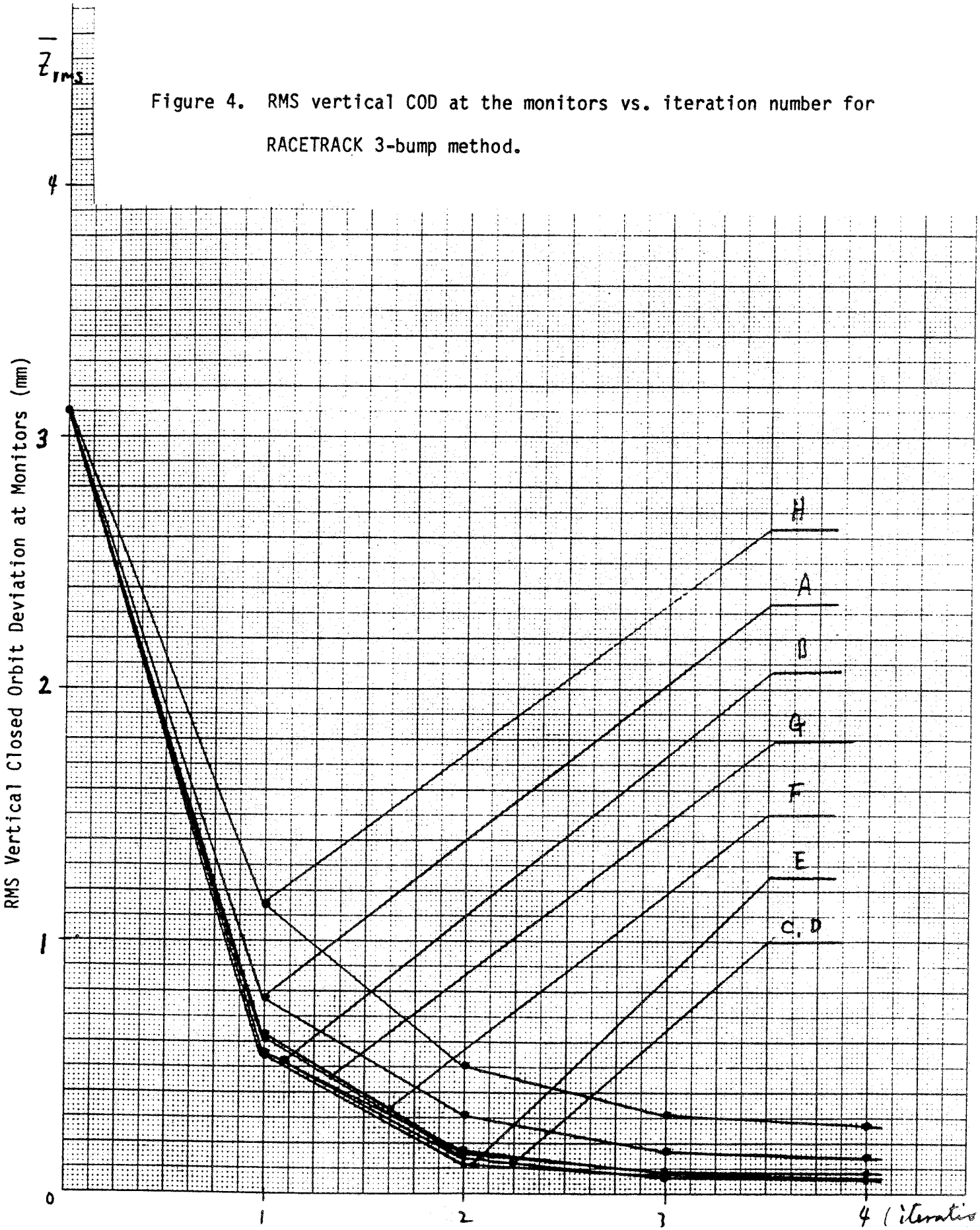

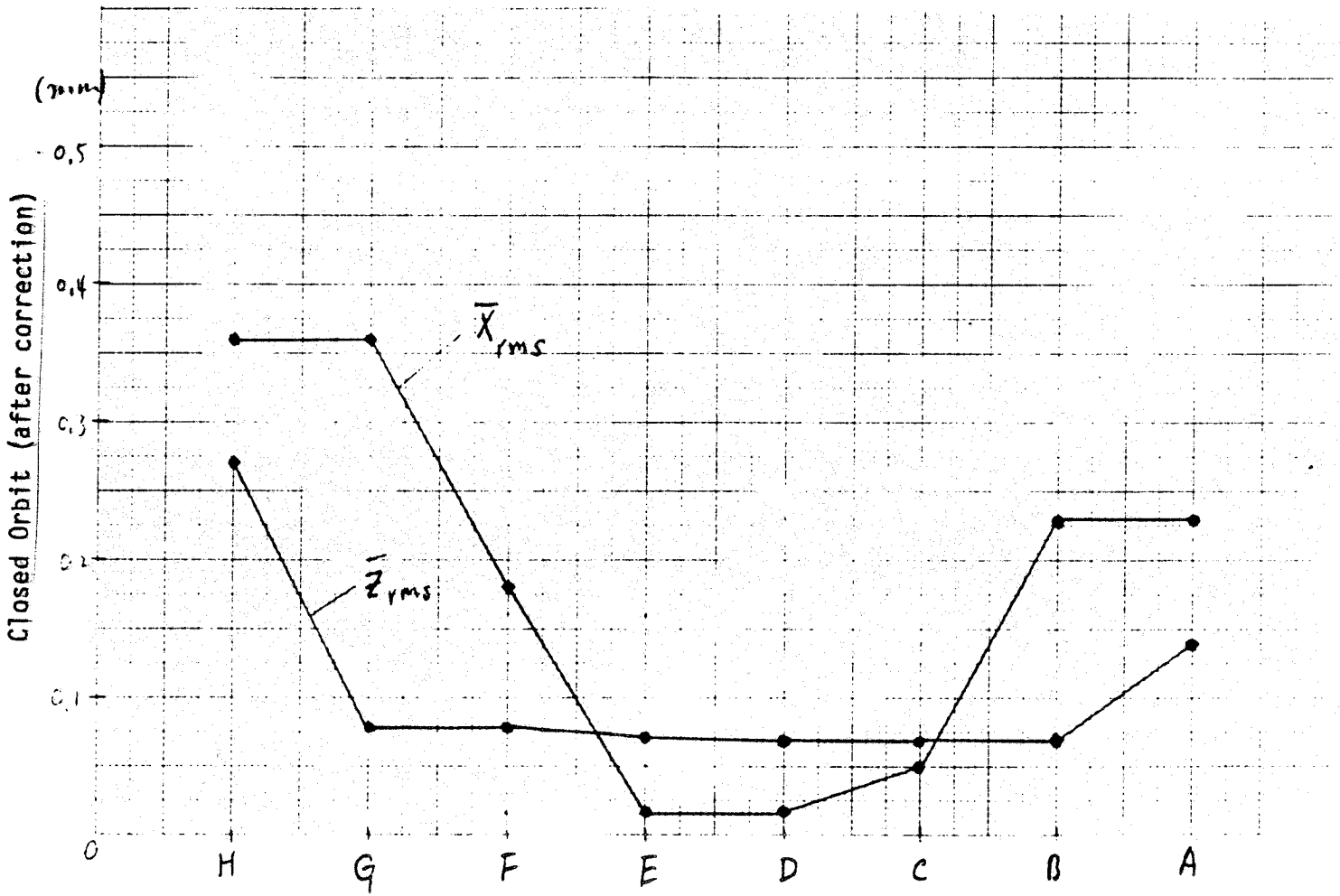

Figure 5. RMS horizontal and vertical COD at the monitors after 4 iterations of the RACETRACK 3-bump method.

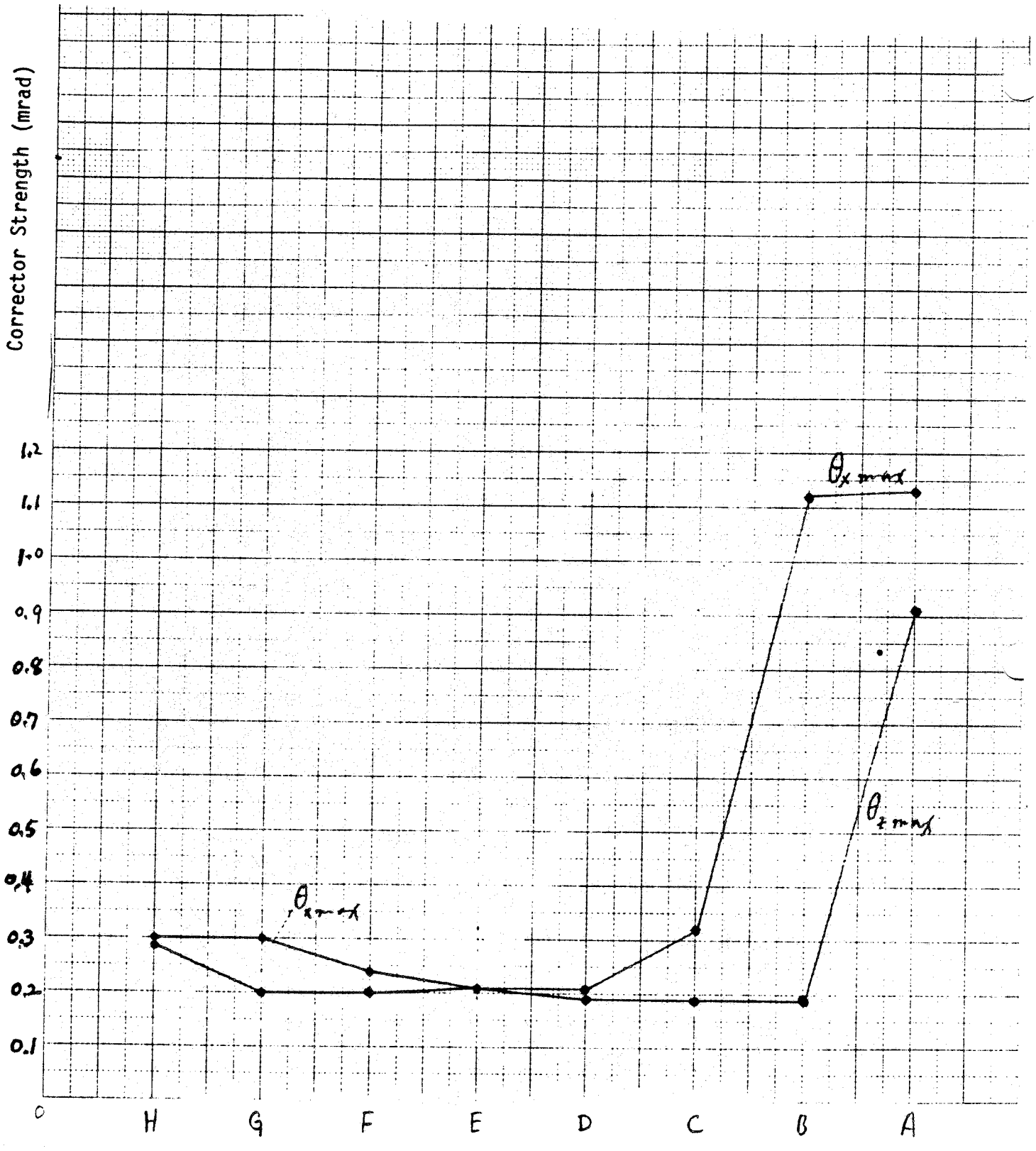

Figure 6. Maximum H and V corrector strength for 4 iterations of the RACETRACK 3-bump method.

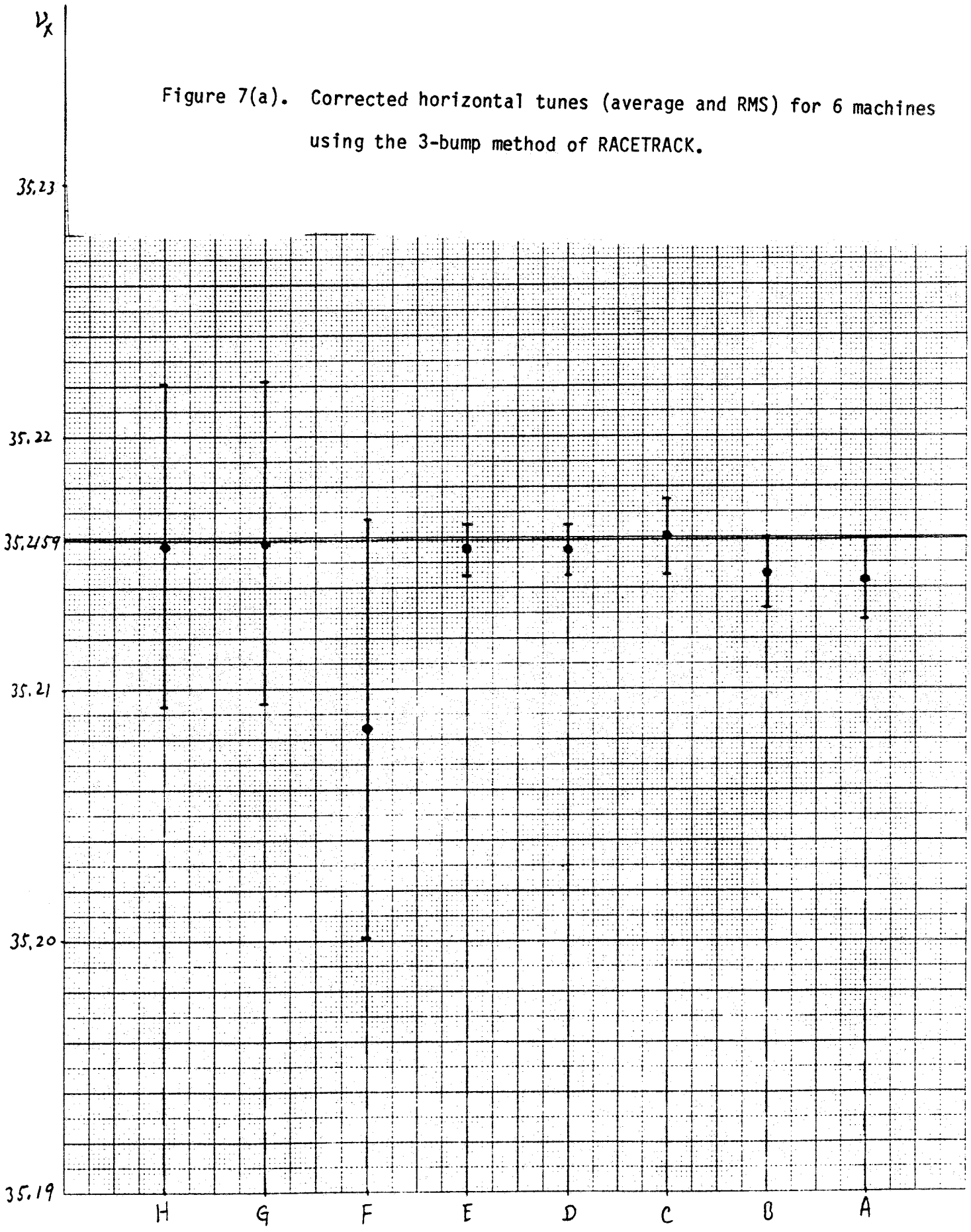

Figure 7(a). Corrected horizontal tunes (average and RMS) for 6 machines using the 3-bump method of RACETRACK.

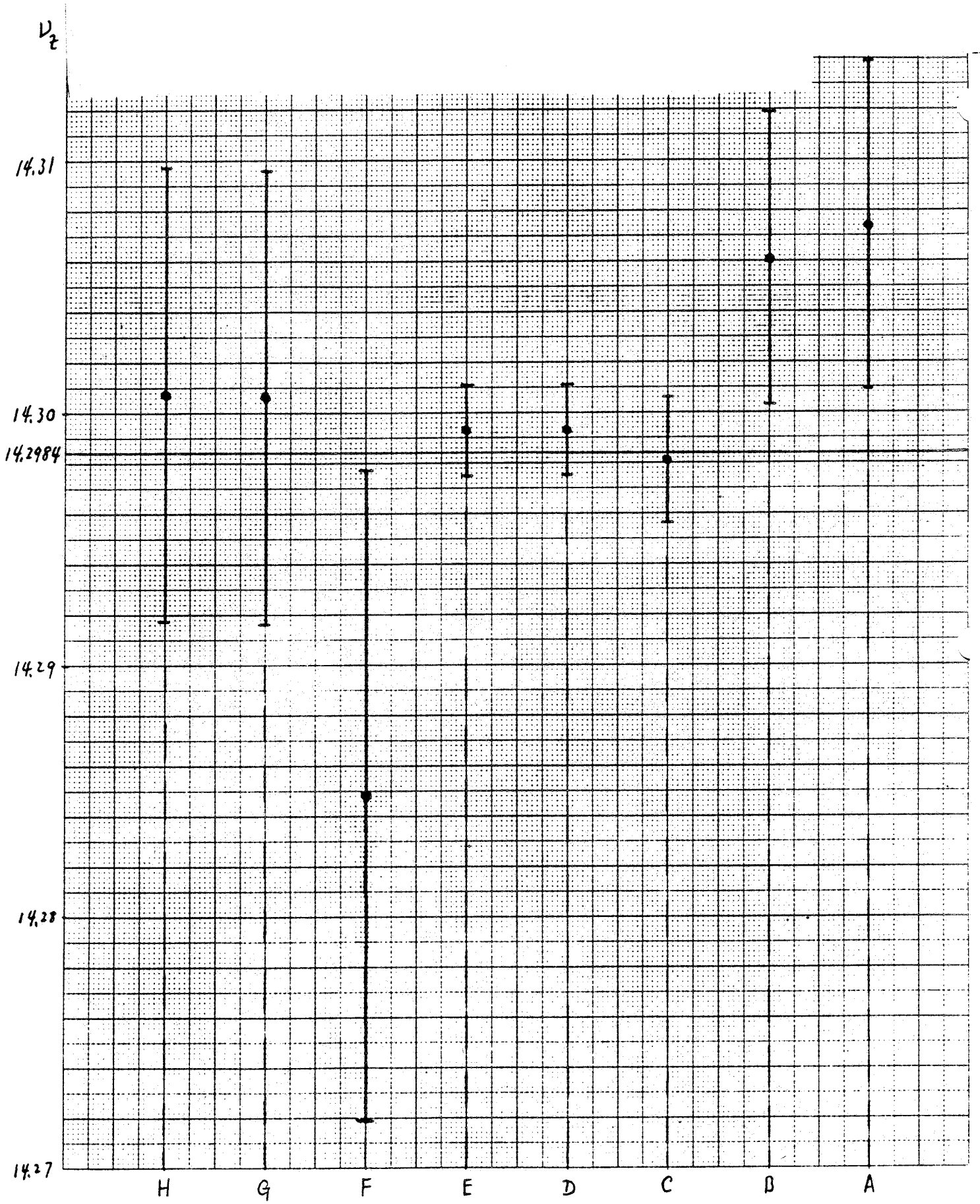

Figure 7(b). Corrected vertical tunes for 6 machines (RACETRACK).

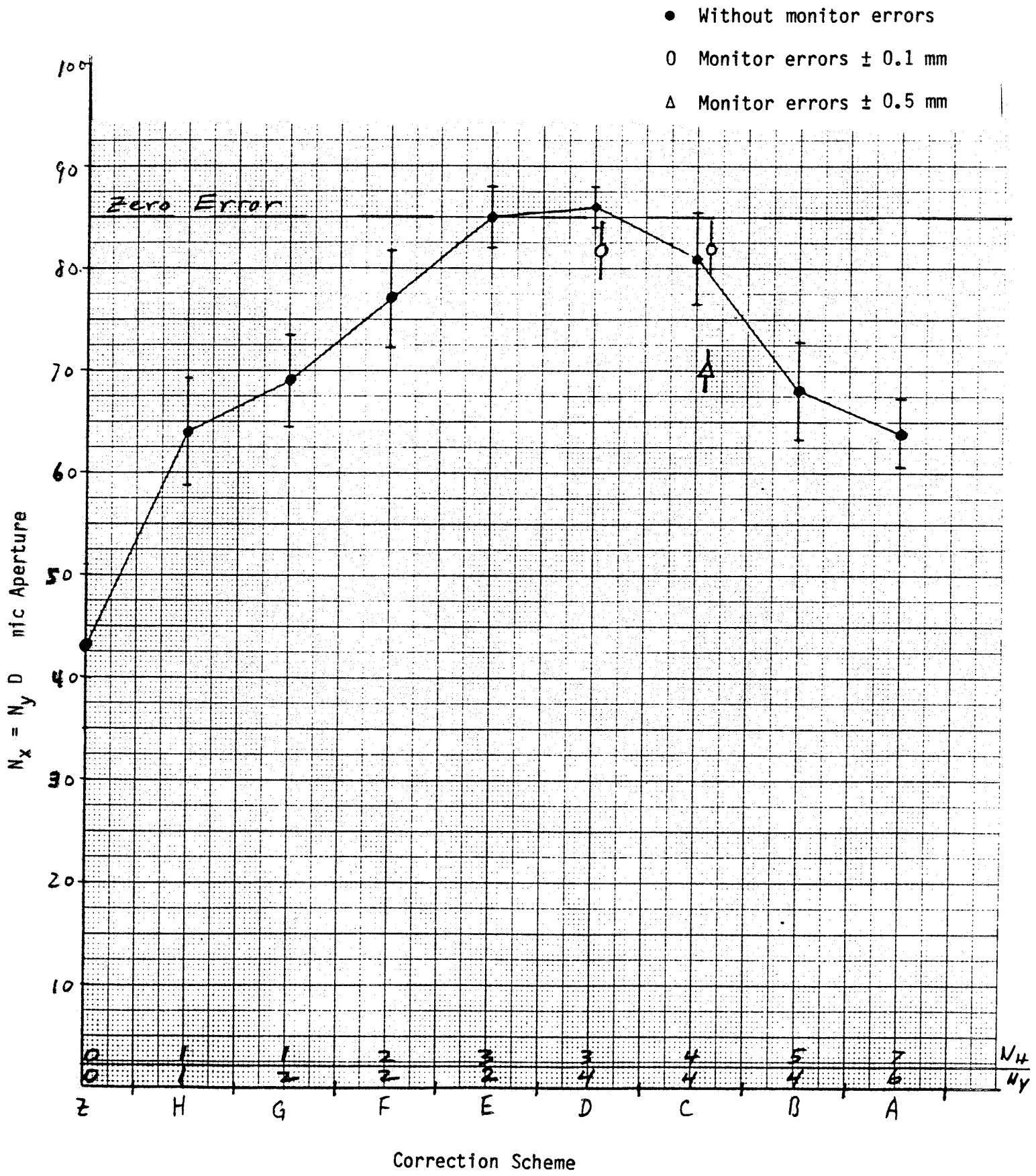

Figure 8. Average and RMS dynamic aperture for 6 machines vs. correction scheme (RACETRACK).

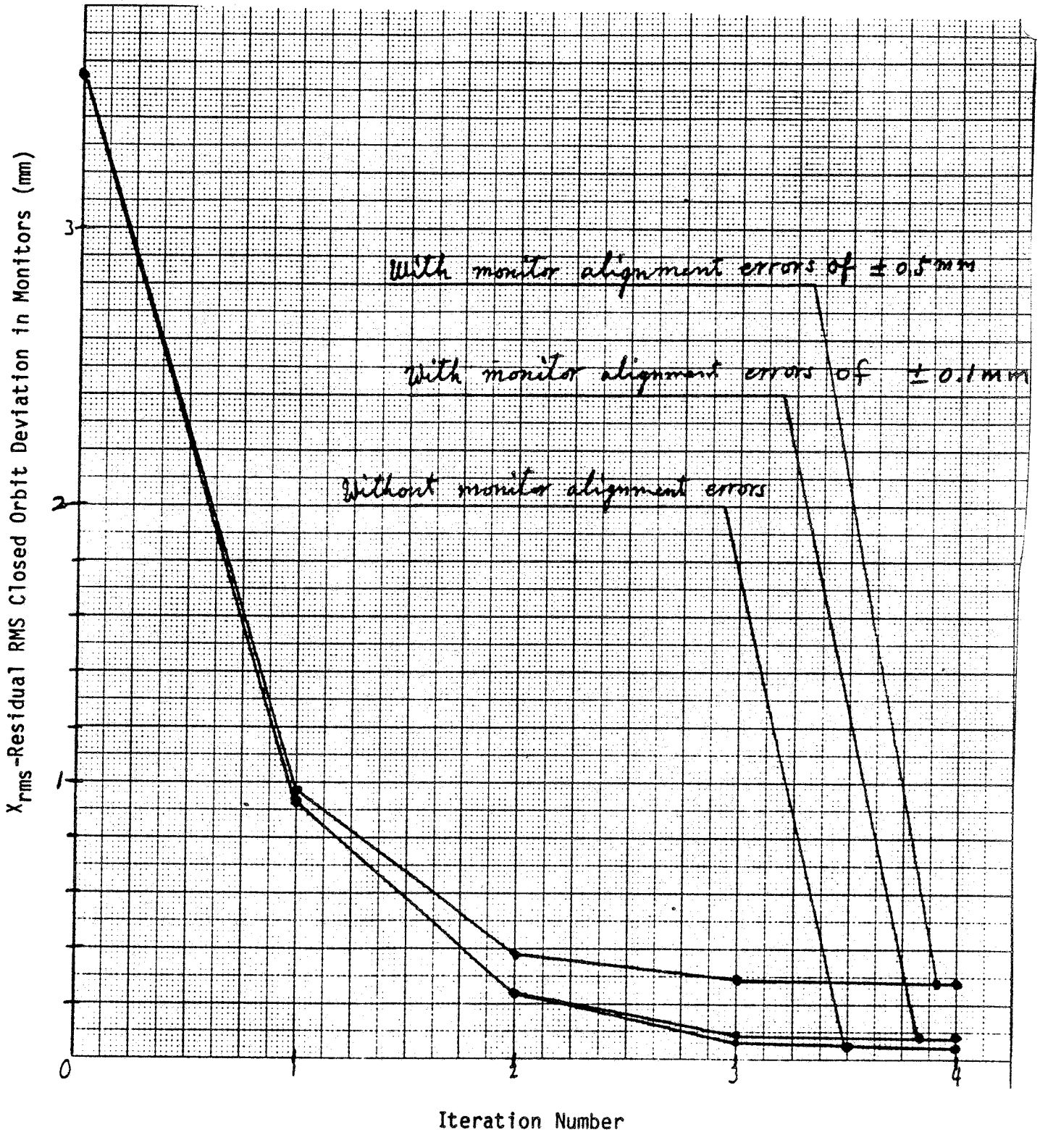

Figure 9. RMS horizontal COD with and without monitor alignment errors (Scheme C)

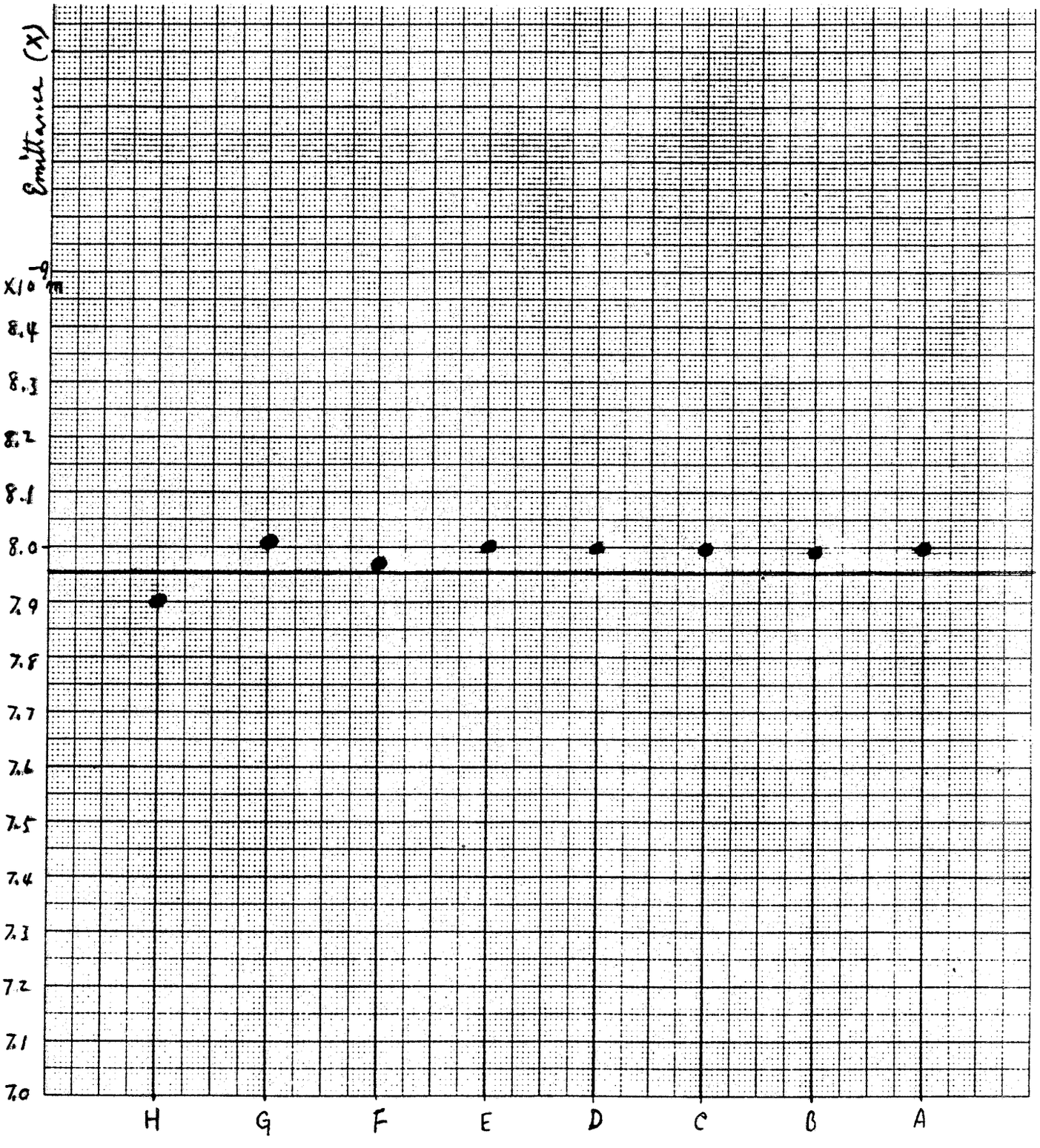

Figure 10. Corrected horizontal emittance for 1 machine using PETROC correction method (MICADO)

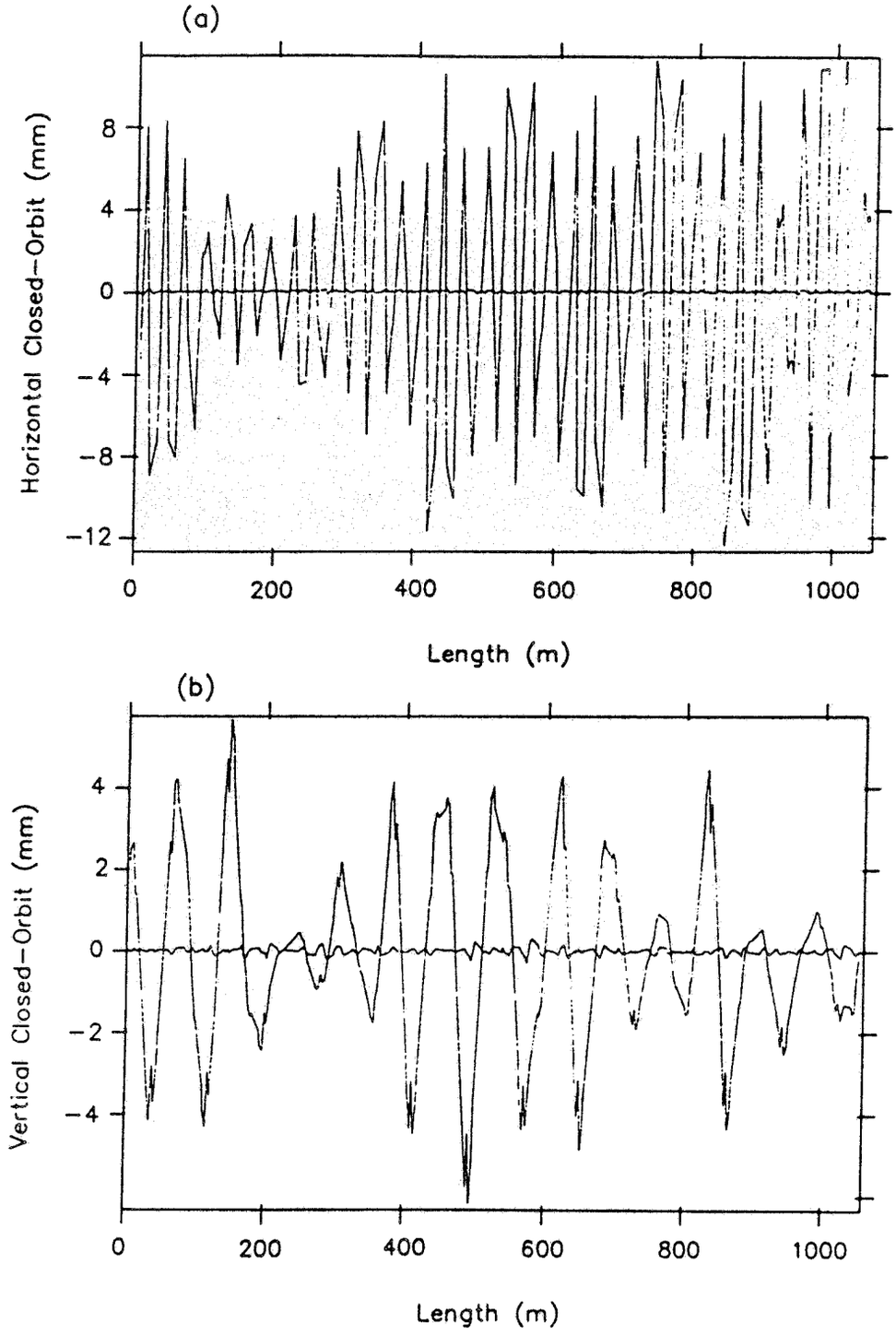

Figure 11.

(a) **Horizontal closed-orbit distortions at the monitors for the entire machine, at a 10^{-4} tolerance level, with and without corrections.**

(b) **Vertical closed-orbit distortions at the monitors for the entire machine, at a 10^{-4} tolerance level, with and without corrections.**

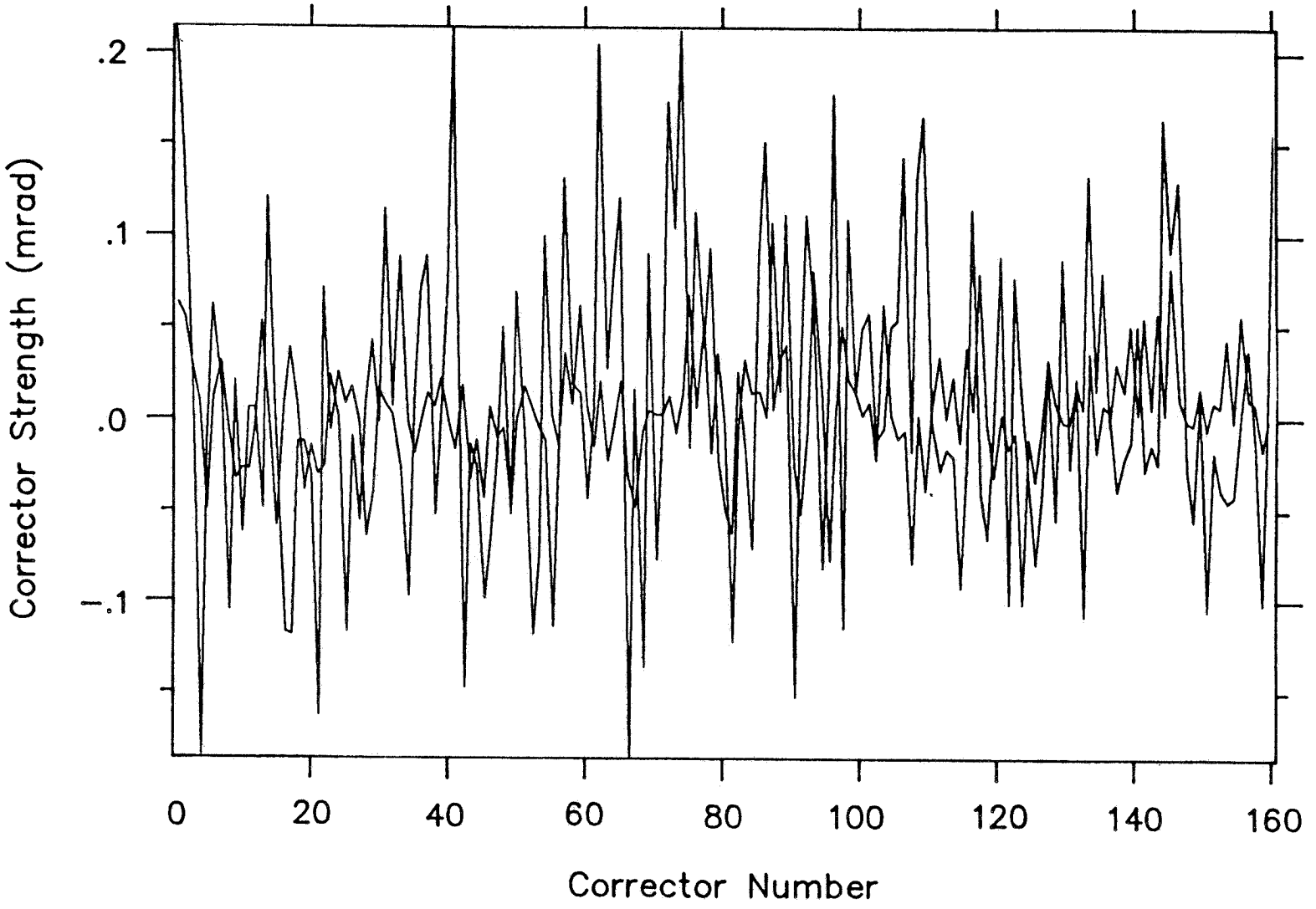

Figure 12.

Horizontal and vertical correction magnet strength in mrad for the corrections shown in Figure // (a and b).